Biomedicine & Pharmacotherapy 165 (2023) 115034

Contents lists available at ScienceDirect

Biomedicine & Pharmacotherapy

journal homepage: www.elsevier.com/locate/biopha

# Alpha-tocopheryl succinate and doxorubicin-loaded liposomes improve drug uptake and tumor accumulation in a murine breast tumor model

Fernanda A. Boratto [a], Eduardo B. Lages [a], Cristina M.C. Loures [b], Adriano P. Sabino [b], Angelo Malachias [c], Danyelle M. Townsend [d], Andre Luis Branco De Barros [b,*], Lucas Antonio Miranda Ferreira [a], Elaine Amaral Leite [a,*]

[a] Department of Pharmaceutical Products, Faculty of Pharmacy, Universidade Federal de Minas Gerais, Belo Horizonte, Minas Gerais, Brazil
[b] Department of Clinical and Toxicological Analyses, Faculty of Pharmacy, Universidade Federal de Minas Gerais, Belo Horizonte, Minas Gerais, Brazil
[c] Department of Physics, Institute of Exact Sciences, Universidade Federal de Minas Gerais, Belo Horizonte, Minas Gerais, Brazil
[d] Department of Drug Discovery and Biomedical Sciences, Medical University of South Carolina, Charleston, SC, United States

ARTICLE INFO

*Keywords:*
Doxorubicin
Alpha-tocopheryl succinate
PH-sensitive liposomes
Tumor accumulation
Breast cancer

ABSTRACT

Liposomes composed of a rigid bilayer have high plasma stability; however, they can be challenged in efficacy due to complications in releasing the encapsulated drug as well as being internalized by the tumor cell. On the other hand, fusogenic liposomes may fuse with the plasmatic membrane and release encapsulated material directly into the cytoplasm. In a previous study, fusogenic liposomes composed of alpha-tocopheryl succinate (TS) and doxorubicin (DOX) were developed (pHSL-TS-DOX). These stabilized tumor growth and reduced toxicity compared to a commercial formulation. In the present study, we investigated whether cellular uptake or DOX accumulation in the tumor could justify the better performance of the pHSL-TS-DOX formulation. Release, deformability, and DOX plasmatic concentration studies were also carried out. pHSL-TS-DOX showed an adequate release profile and demonstrated characteristics of a deformable formulation. Data from apoptosis, cell cycle, and nuclear morphology studies have shown that the induction of cell death caused by pHSL-TS-DOX occurred more quickly. Higher DOX cellular uptake and tumor accumulation were observed when pHSL-TS-DOX was administered, demonstrating better drug delivery capacity. Therefore, better DOX uptake as well as tumor accumulation explain the great antitumor activity previously demonstrated for this formulation.

## 1. Introduction

The anthracycline antibiotic doxorubicin (DOX) has a broad spectrum of activity against different types of cancer and is often used as a single agent or in therapeutic combination regimens [1]. DOX treatment can lead to cardiotoxicity and as such alternative drug delivery strategies have been investigated. Doxil® (Janssen Biotech, Inc., Johnson & Johnson, USA) demonstrated a reduction in cardiotoxicity and myelosuppression, which are severe limitations of the DOX treatment [2–4]. The rationale behind the use of Doxil® was based on (i) prolonging the drug circulation time and avoiding clearance by cells of the mononuclear phagocytic system by using a PEGylated liposome, (ii) high and stable remote loading of DOX driven by a transmembrane ammonium sulfate gradient, and (iii) lipid bilayer composed of the high-Tm (53 °C) saturated phosphatidylcholine [2,5]. Despite all the advantages of Doxil®, other modern strategies in the nanosystems area, whether using polymorphic lipids or techniques of drug encapsulation without using a remote gradient, as well as the association with more than one component that presents antitumor activity, may be beneficial [6].

Our group recently developed a new pH-sensitive liposome containing DOX and alpha-tocopheryl succinate (TS) (pHSL-TS-DOX)[7]. pH-sensitive liposomes have been designed to be less stable in an acidic environment, as the tumor tissue and intracellular endosomes (pH about 6.5 and 5.0–6.0, respectively), than normal tissues (pH 7.4)[7,8]. This system contains a polymorphic lipid capable of forming a lamellar bilayer at physiological pH. When submitted to an acidic environment, it undergoes destabilization and changes to a hexagonal phase, releasing the vesicle content [9,10].

In our previous work, a new and efficient DOX encapsulation method in the absence of ammonium sulfate (a passive loading method) was

* Corresponding authors.
*E-mail addresses:* brancodebarros@yahoo.com.br, albb@ufmg.br (A.L. Branco De Barros), elaineleite@ufmg.br, leite_elaine@hotmail.com (E. Amaral Leite).

https://doi.org/10.1016/j.biopha.2023.115034
Received 24 April 2023; Received in revised form 10 June 2023; Accepted 13 June 2023
Available online 23 June 2023

obtained and showed high encapsulation percentage and improved the DOX release profile. The formulation proved to be more efficient in controlling the tumor growth in a 4T1 breast tumor-induced model than a non-pH-sensitive formulation (similar to Doxil®, npHSL-DOX-AS). Additionally, it was shown to be safe, harmless to the heart and liver, and avoided myelosuppression [7]. All these benefits over a well-established formulation used in the clinic motivate us to pursue further biological studies to a better comprehension of the pharmacokinetic features of this formulation as well as its cellular uptake, tumor accumulation, and possible effects on the cell cycle.

## 2. Materials and methods

### 2.1. Materials

Doxorubicin hydrochloride (DOX) was acquired from ACIC Chemicals (Ontario, Canada). Alpha-tocopheryl succinate (TS) was obtained from Sigma-Aldrich (Steinheim, Germany) as well as cholesterol, ammonium sulfate, 4-(2-hydroxyethyl)− 1-piperazine ethanosulphonic acid (HEPES), and trypsin. Dioleoylphosphatidylethanolamine (DOPE), 1,2-distearoyl-sn-glycero-3-phosphoethanolamine-N-[methoxy(polyethyleneglycol)− 2000] (DSPE-$PEG_{2000}$) and hydrogenated soybean phosphatidylcholine (HSPC)were purchased from Lipoid (Ludwigshafen, Germany). Sodium hydroxide was obtained from Vetec Química Fina Ltda (Rio de Janeiro, Brazil). Chloroform and anhydrous monobasic potassium phosphate were purchased by Synth (São Paulo, Brazil). Methanol (HPLC grade) was obtained from Tedia (Fairfield, USA). 4T1 breast tumor cell line was purchased from ATCC (Manassas, USA). Roswell Park Memorial Institute 1640 (RPMI-1640) medium, fetal bovine serum (FBS), streptomycin, and penicillin were obtained from Invitrogen (São Paulo, Brazil). Ketamine and xylazine were obtained from Vetbrands Agroline (Campo Grande, Brazil) and Hertape Calier Saúde Animal S/A (Juatuba, Brazil), respectively. The other chemicals were of analytical grade.

### 2.2. Liposomes preparation

The pHSL-TS-DOX was prepared by hydration of lipid film as described previously [7]. Chloroform aliquot of DOPE, TS, and DSPE--$PEG_{2000}$ (molar ratio of 55:40:5, and lipid concentration 40 mM) was added into a round bottom flask, and evaporated under reduced pressure to form thin lipid film. NaOH solution was added to the film to promote complete TS ionization. Then, HEPES-saline buffer pH 7.4 (HBS) was added. The obtained vesicles were sonicated using an ultrasonic homogenization apparatus (CPX 500, Cole Parmer, Vernon Hills, USA) with a high-power probe with 21% amplitude for 3 min in an ice bath. The next step was to add 1.0 mL DOX solution (10 mg/mL). After complete homogenization, the dispersion was kept under refrigeration at 4 °C for 2 h.

To evaluate the advantages of pHSL-TS-DOX over a non-pH-responsive liposome, a formulation comparable to a commercially available one was prepared, npHSL-DOX-AS. This formulation made of HSPC:CHOL:DSPE-PEG2000–57:38:5, lipid concentration of 20 mmol/L, was prepared by the film hydration method followed by extrusion, and DOX encapsulation by the ammonium sulfate gradient method for one hour. In both cases, untrapped DOX was eliminated by ultracentrifugation at 350,000 x g, 4 °C for 180 min (OPTIMA L-80XP, Beckman Coulter−Fullerton, CA, USA) and the pellet was resuspended with HBS.

### 2.3. Liposomes characterization

The mean diameter and polydispersity index (PDI) of the liposomes were evaluated by dynamic light scattering (DLS) as previously described [7]. Briefly, the studies were performed 25 °C at a 90° angle using monomodal analysis; the zeta potential value was obtained by DLS associated with the electrophoretic mobility at an angle of 90° using the Zetasizer Nano ZS90 (Malvern Instruments, Malvern, UK).

The DOX concentration in the pHSL-TS-DOX and npHSL-DOX-AS was determined by high-performance liquid chromatography (HPLC) using fluorimetric detection in a Waters chromatographer (Waters Instruments, 1200 series, Milford, USA). Separation was achieved using a 250 × 4.6 mm, 5 μm column (Merck, ACE® 250–4.6 C8, Aberdeen, Scotland), with a flow rate of 1.0 mL/min. Drug was eluted with methanol:phosphate buffer 0.01 M pH 3.0 (65:35 v/v, respectively). The DOX detection was performed at excitation/emission wavelengths of 477/555 nm. The encapsulation percentage (EP) was calculated as the equation below:

$$EP = \frac{[DOX]_{Purified\ \ Lip}}{[DOX]_{Total\ Lip}} \quad (1)$$

**Abbreviations:** EP: encapsulation percentage, $[DOX]_{Purified\ Lip}$: doxorubicin concentration after liposome purification, $[DOX]_{Total\ Lip}$: doxorubicin concentration before liposome purification.

The analyzes were performed in triplicate and were presented as the mean ± standard deviation of at least three batches.

### 2.4. Release studies

One milliliter of the pHSL-TS-DOX, npHSL-DOX-AS, or free DOX was added to a dialysis bag (CelluSep® 14 kDa) along with 1.0 mL of RPMI pH 7.4 supplemented with FBS. The dialysis bag was dropped into an external phase with 25 mL or 50 mL of RPMI pH 7.4 supplemented with FBS under magnetic stirring at 37 °C. Sampling aliquots (1.0 mL) from the external phase were taken (1, 2, 3, 4, 6, 8, and 24 h), and the same fresh medium volume was added. Samples were homogenized with acetonitrile and centrifuged at 9400 x g for 15 min. The supernatant was used for DOX quantification by HPLC. The values obtained were graphically represented as the cumulative percentage of drug release.

### 2.5. Deformability test

The deformability of pHSL-TS and npHSL-AS (both without DOX) was assessed by the modification of the DLS average vesicle size upon extrusion. The formulations were passed once in a polycarbonate membrane of pore size of 100 nm. After the extrusion membrane used was turned 180° and the vehicle of each formulation was passed, making a backwash. Mean diameters of the formulations before and after extrusion as well as the backwash liquid were measured by DLS. We emphasize here that a chain of successive extrusion procedures leads to liposomes with sizes of the used membrane pore, while the study of liposome size after single or few extrusion procedures provides more precise information on actual vesicle deformability. Retention of larger vesicle sizes (observed upon DLS analysis of backwashed membranes) indicates poor elasticity on a given system while a DLS distribution with vesicle sizes close to the target size defined by the membrane pore after a single extrusion indicates improved elasticity of a liposome formulation. A more detailed explanation of the fundamentals of the technique is available in the supplementary material.

### 2.6. In vivo studies

#### 2.6.1. DOX plasmatic concentration studies

*In vivo* studies were conducted under the approval of the local Ethics Committee on Animal Use (CEUA) (Protocol # 63/2019) following the National Institutes of Health Guide for the Care and Use of Laboratory Animals. All institutional and national guidelines for the care and use of laboratory animals were followed. Groups of four healthy BALB/c female mice (22 – 25 g) received a dose equivalent to 5 mg/kg of DOX. The treatments were as follows: free DOX, pHSL-TS-DOX, and npHSL-DOX-AS *via* the tail vein injection. At 1, 4, and 24 h post-injection, blood was collected from anesthetized mice by puncture of the

brachial plexus in tubes containing an anticoagulant (0.18% w/v EDTA) [11]. Then, the blood was centrifuged (1200 x g, for 10 min), and the plasma obtained was used for DOX quantification by HPLC. The samples were diluted before the analysis as follows: 125 μL of plasma of mice were added to an Eppendorf tube with daunorubicin (internal standard) and 150 μL of acetonitrile. The suspensions were homogenized and centrifuged at 9400 x g for 15 min. The supernatants containing the extracted DOX were used for quantification. A six-point standard curve (10, 100, 200, 300, 400, and 500 ng/mL) *vs*. area under curve ratio DOX/daunorubicin was previously prepared using plasma of mice. Data obtained by linear regression were $y = 0.0033\ x + 0.0557$ and $r^2 = 0.9781$.

#### 2.6.2. Quantification of DOX in the tumor

BALB/c female mice (22 – 25 g) received, subcutaneously, into the left thigh, aliquots (100 μL) of $1.0 \times 10^6$ 4T1 cells in RPMI. After eleven days of inoculation, mice were randomly divided into three groups (n = 4). The animals received a single dose (the equivalent to 20 mg/kg of DOX) of free DOX, pHSL-TS-DOX, or npHSL-DOX-AS *via* the tail vein. At 4 h post-injection, the animals were anesthetized and euthanized by blood puncture, and then the tumors were collected and weighted. Then, tumors were homogenized with 300 μL of acetonitrile in Ultra Turrax T-25 homogenizer (Ika Labortechnik, Germany) and 50 μL of Triton X-100 10% v/v, 50 μL of distilled water and 300 μL of acidified isopropanol (0.75 N) were added [12]. The preparation was maintained overnight at − 20ºC for DOX extraction. Afterward, samples were warmed to room temperature, vortexed for 5 min, and centrifuged at 9400 x g for 15 min. For DOX quantification by HPLC, 125 μL of the supernatant obtained were added to an Eppendorf tube with daunorubicin (internal standard) and 150 μL of acetonitrile.

### 2.7. In vitro studies

#### 2.7.1. Cell culture

4T1 cell line (murine breast tumor) was cultured with RPMI-1640 medium and supplemented with FBS (10% v/v), penicillin (1% w/v), and streptomycin (1% v/v). The cells were kept on a humidified incubator with 5% $CO_2$ at 37 °C until they reach confluency and subcultured.

#### 2.7.2. Cellular uptake

4T1 cells ($1 \times 10^6$ cells/well) were seeded in 12-well plates and maintained at 37 °C and 5% $CO_2$. After 24 h, the culture medium was removed, and cells were treated with free DOX, pHSL-TS-DOX, and npHSL-DOX-AS (DOX concentration of 1 μM) and incubated for 1, 2, or 8 h. After incubation, the medium was removed, and the cells were washed with PBS. Then, the cells were trypsinized, homogenized, and centrifuged at 160 x g for 5 min. The *pellet* was resuspended with 1.0 mL of isopropanol:methanol (1:4 v/v). The dispersion was submitted to homogenization in an ultrasound bath for 15 min, centrifuged at 1200 x g for 15 min. The supernatant was used for DOX quantification by HPLC. The cellular uptake was calculated by the ratio of the DOX obtained in the quantification of each well and the DOX used in cell treatment (1 μM).

#### 2.7.3. Analysis of apoptosis

Initially, 4T1 cells were seeded on a 12-well plate and incubated at 37 °C and 5% $CO_2$ in a density of 300,000 cells/well. After incubation, free DOX, pHSL-TS-DOX, and npHSL-DOX-AS were added to the wells at a DOX concentration of 1 μM or 2 μM. After 4 or 8 h, the culture medium was removed, and the cells were washed with PBS buffer, trypsinized, homogenized with RPMI, and centrifuged for 5 min at 160 x g. Under the *pellet* was added the binding buffer, 2.5 μL of Annexin V solution, and 2.5 μL of Propidium iodide (PI) (Annexin V - FITC Apoptosis Detection Kit – Sigma Aldrich). The plate was incubated for 20 min protected from light. A total of 50,000 events was recorded, and the analysis was performed on a flow cytometer (LSR Fortessa BD Biosciences) according to the manufacturer's instructions.

#### 2.7.4. Analysis of cell cycle

4T1 cells were seeded (300,000 cells/well) on a 12-well plate and incubated for 24 h at 37 °C and 5% $CO_2$. After incubation, free DOX, pHSL-TS-DOX, and npHSL-DOX-AS were added to the wells at a DOX concentration of 1 μM. After 8 h, the culture medium was removed, and the cells were washed with PBS buffer, trypsinized, homogenized with RPMI, and centrifuged for 5 min at 160 x g. The pellet was homogenized with 1 mL of ethyl alcohol 70% v/v and incubated for 30 min at 4 °C. Then, the cells were centrifuged for 5 min at 290 x g, and the *pellet* was resuspended with a solution containing RNAse, PI, and PBS. The cell dispersion was incubated for 15 min at 37 °C and protected from light. A total of 50,000 events was recorded on a flow cytometer (LSR Fortessa BD Biosciences) according to the manufacturer's instructions.

#### 2.7.5. Nuclear morphometric analyses

4T1 cells were plated at a density of $2.5 \times 10^5$ cells/well in 6-well plates and incubated at 37 °C for 24 h. The cells were treated with free DOX, pHSL-TS-DOX, or npHSL-DOX-AS (1 μM) for 24 h [13]. Afterward, the cells were fixed with formaldehyde 3.7% (v/v) for 10 min and stained with Hoescht 33342 (0.2 μg/mL) solution for 10 min protected from light. The fluorescence images of nuclei were captured using a microscope AxioVert 25, with a fluorescence module Fluo HBO 50 connected to the Axio Cam MRC camera (Zeiss, Oberkochen, Germany). A total of 100 nuclei per treatment was analyzed using the Software Image J 1.50i (National Institutes of Health, Bethesda, USA) and the plugin "NII_Plugin" available at http://www.ufrgs.br/labsinal/NMA/.

### 2.8. Statistical analysis

The normality of variance was evaluated by the Kolmogorov-Smirnov or D'Agostino and Pearson test. The variables which did not follow normal distribution were transformed as: y = log or y = log (variable +200). The experimental groups' difference between each other was tested by one-way ANOVA followed by Tukey's test. It was considered a confidence range of 95%, and differences were considered significant when the p-value was less than 0.05 ($p < 0.05$).

## 3. Results

### 3.1. Liposomes characterization

The average diameter for pHSL-TS-DOX and npHSL-DOX-AS was 164 ± 22 nm (PDI 0.23 ± 0.06), and 142 ± 15 nm (PDI 0.05 ± 0.03), respectively, indicating monodisperse vesicles population (< 0.3). Zeta potential values were close to neutrality (- 2.7 ± 0.8 mV and −2.2 ± 1.0 mV) as expected, due to the presence of $DSPE\text{-}PEG_{2000}$ [14]. A high DOX encapsulation content (97.2 ± 9.0% and 98.4 ± 6.0%) could be achieved in both cases.

The pHSL-TS-DOX and npHSL-DOX-AS were assessed for *in vitro* DOX release at pH 7.4 in RPMI. The data shown in Fig. 1 illustrates that pHSL-TS-DOX showed a sustained release profile. The percentage of released DOX increased with time, reaching a maximum release of around 25% after 24 h. By contrast, DOX release from npHSL-DOX-AS was much lower than observed for pHSL-TS-DOX and the rate of release remained practically constant (around 2%) throughout the study. The free DOX dissolution profile was also analyzed for comparison. After 2 h, 100% of the DOX has already dissolved.

A deformability study was performed (Fig. 2A), and showed a heterogeneous distribution of average diameters could be observed for pHSL-TS and npHSL-AS formulations before extrusion (blue line and red line, respectively). It is worth noting that very large vesicles are present in the npHSL-AS sample, with an intense peak observed around 6000 nm vesicle size. The abrupt asymmetry on the peak shape is ascribed to an intrinsic limitation of the DLS measurements, which are unable to detect

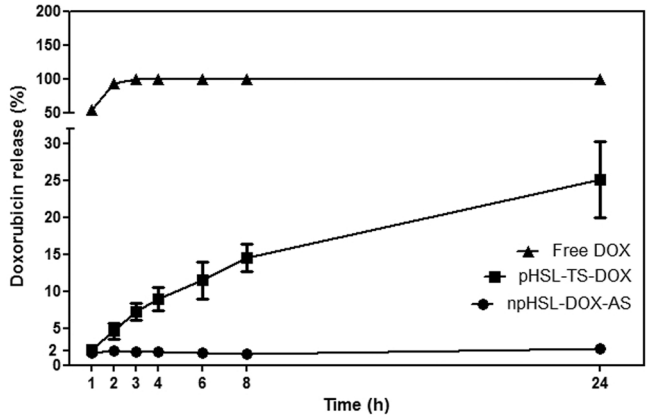


**Fig. 1.** In Vitro Drug Release. Doxorubicin release at pH 7.4 in RPMI. Results expressed as the mean ± SD (n = 3).

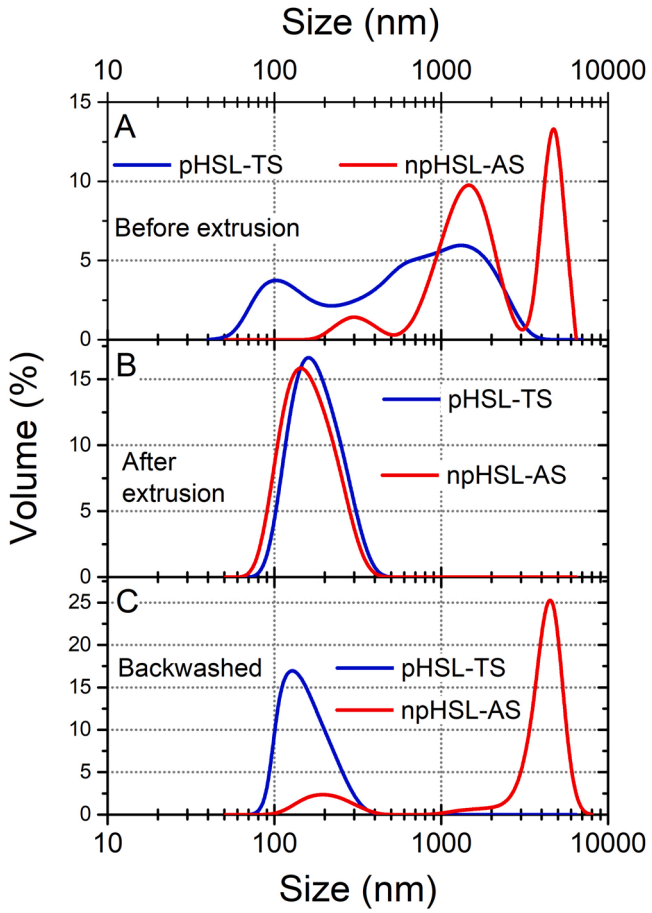


**Fig. 2.** In Vitro Structural Characterization. Representative profile of size distribution of pHSL-TS and npHSL-AS evaluated before extrusion (A and B), after extrusion (C and D) and in backwash (E and F) by DLS analysis.

objects with sizes larger than 8000 nm for the wavelength used. After a single extrusion, both formulations showed a peak centered near 150 nm (Fig. 2B), which corresponds to extruded liposomes of pHSL-TS and npHSL-AS formulations. In the backwash analysis of npHSL-AS, inverting the inlet direction of the membrane, distinct behaviors could be observed (Fig. 2C). A single peak was retrieved for the pHSL-TS formulation, while two populations were detected for the npHSL-AS sample. In this latter case, the peak observed near 5000 nm represents approximately 74% of the particles. This result suggests that the majority of npHSL-AS liposome vesicles were unable to cross the membrane after a single extrusion process. On the other hand, the pHSL-TS size distribution indicates the possibility of achieving a completely deformed system with pore-induced vesicle size after a single extrusion.

### 3.2. DOX plasmatic concentration studies

To assess the pharmacokinetic properties of the preparations, we performed a DOX plasma concentration study in healthy mice treated with free DOX, pHSL-TS-DOX, or npHSL-DOX-AS, as shown in Fig. 3A. Plasma concentration of free DOX and pHSL-TS-DOX showed values ranging from $4.80 \times 10^{-2} \pm 0.76 \times 10^{-2}$ μg/mL and $2.92 \times 10^{-2} \pm 0.37 \times 10^{-2}$ μg/mL at 1 h to $0.11 \times 10^{-2} \pm 0.02 \times 10^{-2}$ μg/mL and $0.16 \times 10^{-2} \pm 0.03 \times 10^{-2}$ μg/mL at 24 h respectively. In contrast, npHSL-DOX-AS reached a higher plasma DOX concentration throughout the experiment: 63.02 ± 1.54 μg/mL at 1 h to 0.33 ± 0.27 μg/mL at 24 h.

### 3.3. Tumor accumulation

A major hindrance to drug efficacy is failure to be taken up in the target tissues *in vivo*. Here we evaluated the drug accumulation within tumor tissues in a murine model of breast cancer. Fig. 3B represents the tumor accumulation of DOX. Tumors extracted from mice treated with pHLS-TS-DOX showed that DOX concentration was 2.4 and 1.9-fold higher than npHLS-DOX-AS and free DOX, respectively ($p < 0.05$). On the other hand, no significant difference was observed between free DOX and npHSL-DOX-AS.

### 3.4. Cellular uptake

The cellular uptake study evaluated the DOX concentration upon cell internalization after 1, 2 or 8 h of incubation (Fig. 4). Both DOX and pHSL-TS-DOX showed similar profiles in all times investigated. DOX maximum uptakes of 21.4% ± 3.4, for free DOX, and 20.2% ± 1.9, for pHSL-TS-DOX, were obtained after 8 h of treatment. The treatment with npHSL-DOX-AS induced less DOX internalization in all studied times compared with the other treatments ($p < 0.05$). Its maximum DOX uptake (1.2% ± 0.3) occurred at 2 h.

### 3.5. Apoptosis analysis

The quantification of apoptosis was assessed by flow cytometry with FITC-Annexin V and PI labeling. Murine breast cancer cells were treated with DOX (1 μM) for 8 h. In this study, the level of early apoptosis between the treatments was similar, while the late apoptosis showed to be more intense in free DOX and pHSL-TS-DOX than npHSL-DOX-AS (Figure 1 - Supplementary material). The dose- and time- dependent observations were consistent when 2 μM of DOX and 4 h of incubation were used. However, in this condition, the difference between the late apoptosis of free DOX and pHSL-TS-DOX (14.3% and 15.6%, respectively) and npHSL-DOX-AS (0.72%) was more expressive.

### 3.6. Cell cycle analysis

The impact of the drug formulations on cell cycle was assessed by flow cytometry. The cell cycle distribution in free DOX and pHSL-TS-DOX was close (G1: 55.9% and 61.9%, S: 17.1% and 18.7%, G2-M: 18.0% and 12.9%, respectively). The cells treated with npHSL-DOX-AS showed a different pattern in blocking cell division (G1: 36.7%, S: 21.3% and G2-M: 30.6%); thus, balanced distribution between the cell division stages was observed.

### 3.7. Nuclear morphology

Nuclear morphology was assessed after treatment with DOX, pHSL-

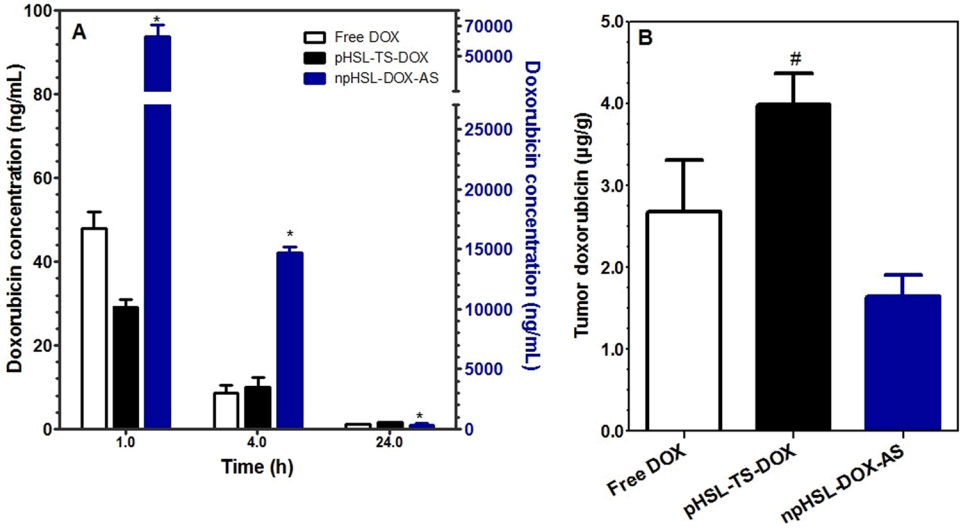


**Fig. 3.** – In Vivo Plasma Concentrations. (A) Evaluation of DOX concentration in plasma after administration of free DOX, pHSL-TS-DOX, and npHSL-DOX-AS. The scale of free DOX and pHSL-TS-DOX should be verified on the left Y-axis; while for npHSL-DOX-AS should be verified on the right Y-axis. (B) DOX concentration in tumor evaluated 4 h after administration of free DOX, pHSL-TS-DOX, and npHSL-DOX-AS. Results expressed as the mean ± SD (n = 4). *Represents significant difference compared to other groups; # Represents significant difference compared to free DOX and npHSL-DOX-AS ($p < 0.05$). The analyses were performed by one-way ANOVA followed by Tukey's test.

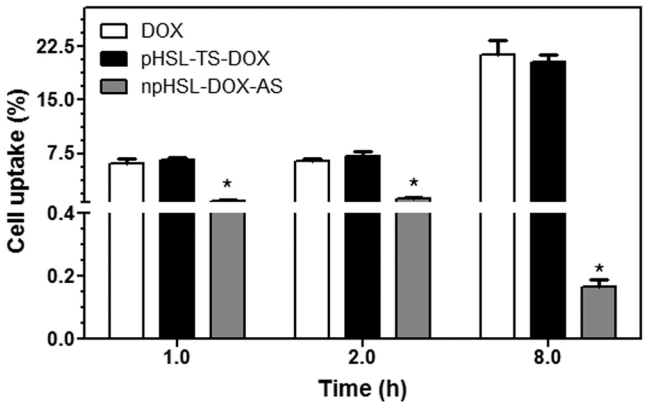


**Fig. 4.** Cellular drug uptake. Percentage of DOX uptake in 4T1 cells treated with free DOX, pHSL-TS-DOX, and npHSL-DOX-AS evaluated after 1, 2 or 8 h of incubation. *Represents significant difference against DOX and pHSL-TS-DOX ($p < 0.05$). Analyses performed by one-way ANOVA followed by Tukey's test.

TS-DOX, and npHSL-DOX-AS according to the "Nuclear Morphometric Analysis Tool" developed by Filippi-Chiela et al. [15]. In this approach six patterns of nuclear morphology related to biological events are defined as follows: normal (N), irregular (I, mitotic catastrophe or other nuclear damaging events), small regular (SR, apoptosis), small (S, mitosis), small irregular (SI, mitosis with damage or nuclear fragments), large regular (LR, senescence), and large irregular (LI, mitotic catastrophe or other nuclear damaging events). Free DOX and pHSL-TS-DOX showed similar percentages of normal nuclei, 20 ± 3% and 25 ± 3%, respectively, while only 5 ± 3% could be observed for npHSL-DOX-AS ($p < 0.05$). Similar percentages of LR nuclei, indicative of senescence, were obtained for free DOX and pHSL-TS-DOX (67 ± 3% and 56 ± 5%, respectively), while it was detected 82 ± 5% of LR nuclei after npHSL-DOX-AS treatment ($p < 0.05$). All treatments resulted in similar percentages of LI + I nuclei, around 15% (Fig. 5A). Fig. 5B presents fluorescence photomicrographs of 4T1 stained nuclei. Control group showed the presence of smaller nuclei with uniform sizes and shapes. Free DOX and pHSL-TS-DOX groups presented some rounded nuclei as well as some elliptic with similar sizes, and npHSL-DOX-AS presented larger nuclei compared to the other groups.

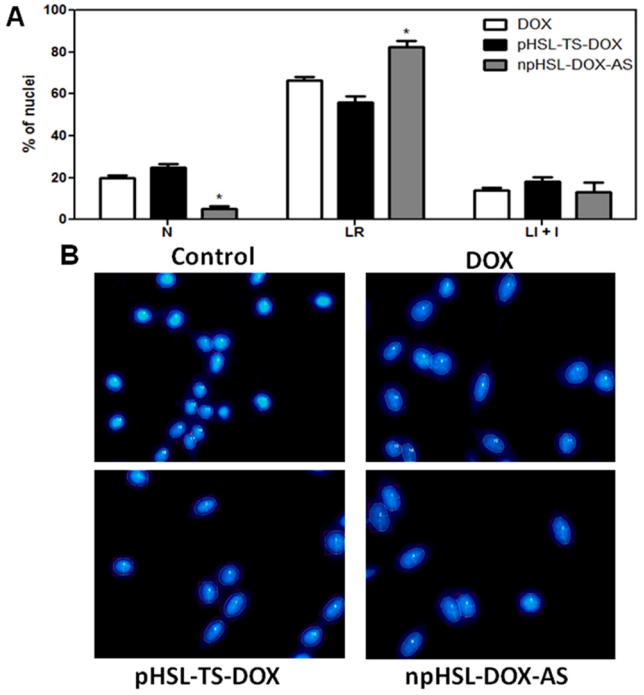


**Fig. 5.** Changes in nuclear morphology following drug treatment. (A) Nuclear morphometric distribution of 4T1 nuclei submitted to different treatments for 24 h. Data represents mean ± SD (n = 3). *Represents significant difference against DOX and pHSL-TS-DOX ($p < 0.05$). Analyses performed by one-way ANOVA followed by Tukey's test. (B) Fluorescence photomicrographs of 4T1 stained with Hoescht 33342 after different treatments. Amplification 40x.

## 4. Discussion

In our previous work, we developed a new pH-sensitive liposomal formulation containing TS and DOX for breast tumor treatment. This formulation was able to promote the tumor growth stabilization in a murine breast tumor model and demonstrated a better safety profile since it did not induce cardiac and hepatic toxicity as well as myelosuppression, the main limitations in DOX use. These parameters were compared with a formulation already used in the clinic (npHSL-DOX-AS, which has the same Doxil® composition), and pHSL-TS-DOX showed superior performance [7]. Given these results, it became interesting to

investigate what factors could contribute to making pHSL-TS-DOX more advantageous. As both formulations contained PEG in the composition, which would confer long circulation time and similar physicochemical characteristics (mean diameter, PDI, zeta potential, and percentage of DOX encapsulation), our first hypothesis focused on investigating the pharmacokinetic profile of these formulations administered to healthy mice. DOX concentration obtained in plasma of animals treated with npHSL-DOX-AS was substantially higher than that observed for free DOX and pHSL-TS-DOX at all times studied (Fig. 3A). After 24 h post-injection, the DOX plasma concentration was 200-times higher from the animals treated with npHSL-DOX-AS than that obtained for pHSL-TS-DOX. The substantially increased amount of plasmatic DOX after npHSL-DOX-AS administration has been described. Gabizon et al. reported a significant increase in AUC (60-fold) and plasma concentration of DOX (hundred-fold) in animals treated with the liposomal drug compared with the free drug many hours after injection [16]. Besides, the AUC (21.60-fold) and half-time life (4.51-fold) of a formulation similar to Doxil® were higher than PEGylated liposomal formulation containing an ion pair between DOX and CHEMS [17]. This difference was related to the insoluble form of the drug inside the liposomal formulation similar to Doxil®, which could minimize the intraliposomal osmotic pressure and help to maintain the liposome integrity, avoiding DOX release. In pHSL-TS-DOX, we postulated that DOX forms an ionic pair with TS and it is soluble and more available to be released, favoring its elimination from the blood.

Unlike the results obtained in plasma, there was a higher tumor accumulation of DOX in animals treated with pHSL-TS-DOX than npHSL-DOX-AS ($p < 0.05$), as demonstrated in Fig. 3B. This finding could explain a better performance in the antitumor activity previously shown for pHSL-TS-DOX [7]. Given each are pegylated formulations with similar diameters and PDI, both would have the same capacity to accumulate in the tumor. Collectively these results suggest that npHSL-DOX-AS remained intact for a longer time in the bloodstream, causing higher DOX plasma levels; however, it could not reach the tumor region in an adequate concentration to exert its antitumor activity, either due to inefficient internalization or release of the drug. Sindhwani et al. demonstrated that 97% of nanoparticles are internalized in the tumor by active trans-endothelial transport and not only by passive transport (EPR effect) [18]. For this transcytosis process, a fusion of endothelial cell membrane with the liposomal membrane is needed. As npHSL-DOX-AS has a very rigid lipid bilayer and hinder the internalization process. The rigidity of the npHSL-DOX-AS liposomal membrane is related to the structural lipid. The long saturated fatty acyl chains of HSPC interact themselves by van der Waals interactions resulting in a high degree of packaging, which requires more energy to break it and explains its high phase transition temperature[2]. Lipids with high phase transition temperatures (above 37 °C) can result in less fluid and leaky lipid bilayers [19]. Higher DOX tumor accumulation after pHSL-TS-DOX treatment than free DOX ($p < 0.05$) was observed. Several factors can explain this finding, such as i) higher level of free DOX clearance suggested by red-colored urine in this group, differently from other treatments; ii) long circulation of pHSL-TS-DOX due to the presence of PEG; iii) high tumor vascularization promotes more uptake of pHSL-TS-DOX by transcytosis. However, this result conflicts with those obtained in the plasma concentration study, in which both treatments reached comparable DOX concentration levels. One hypothesis is that the DOX could be distributed between the blood peripheric tissues and tumor, which has an extensive newly formed vascular network that has a high capacity to capture drug delivery systems [21].

In agreement with the release study, pHSL-TS-DOX showed a higher DOX release compared to npHSL-DOX-AS and presented a sustained drug release during the study. After 24 h of analysis, around 25% of the drug was released from pHSL-TS-DOX, while only 2% from the npHSL-DOX-AS. The lipid composition of pHSL-TS-DOX could bring a more fluid membrane, contributing to more permeability through the lipid bilayer. In fact, in our previous work, we detected 100% of the drug released from pHSL-TS-DOX in HBS buffer at pH 5.0, proving its pH sensitivity [7]. The deformability test data are also in agreement with this hypothesis. For pHSL-TS, the presence of a homogeneous peak around 200 nm after extrusion and in the backwash chart suggests that the pHSL-TS composition caused a higher degree of vesicles flexibility and deformability since the particles were able to break down into smaller particles after passing through the membrane, resulting in a monodisperse population of small vesicles. On the other hand, npHSL-AS extrusion results showed a homogeneous monodisperse distribution peak around 200 nm after extrusion, with retention of larger and undeformed vesicles with an average size of 5000 nm. Such particles could not be deformed and were retained on the extrusion membrane. These results suggest that pHSL-TS exhibit a more elastic (less rigid) bilayer configuration, justifying the improved ability to release DOX properly. The larger relative rigidity of the npHSL-DOX-AS liposomal membrane is likely related to the structural lipid configuration as the HSPC molecules are compactly arranged, leading to a higher degree of packaging [2]. Based on these findings, we can infer that both the rigidity in the lipid bilayer and the presence of DOX as the insoluble salt represent obstacles for the drug release and reduced tumor uptake, consequently resulting in a less effective antitumor activity *in vivo* for npHSL-DOX-AS.

The cellular uptake study results further support a compromised capacity of npHSL-DOX-AS to be internalized by the tumor cell since the rate of DOX uptake after treatment with this formulation was minimal. In contrast, pHSL-TS-DOX showed a maximum DOX uptake (around 20%) after 8 h of treatment, demonstrating its greater drug delivery capacity at the intracellular level. DOPE, structural lipid in this formulation, has fusogenic propriety, which could facilitate the cell internalization of the liposome [20]. This component could allow the fusion between the lipid bilayer and the cell membrane [22]. The low hydration of its polar head group increases the lipophilicity of the liposomal membrane and reduces the energy of interaction between lipid bilayers [23]. Kolasinac and coworkers (2018) studied different compositions of fusogenic liposomes and proved that DOPE has a high ability to fuse with the cell membrane since it was observed a homogenous distribution of the green, fluorescent signal in the cytoplasm of Chinese hamster ovary cells by fluorescence microscopy. A flow cytometry study showed higher fusion efficiency of DOPE (87%) compared to DOPC (7%), which has a bulkier polar group [20]. Despite the fusogenic property of DOPE, we can also consider that another uptake mechanism could occur in some extent, through endocytosis, followed by the destabilization of the liposome at the endosomal level and subsequent release of its content [10]. It is also worth noting that although the amount of released DOX from its free form was undoubtedly superior to that provided by the formulation, the cellular uptake of both was the same (Figs. 1 and 4). The internalization of DOX in the liposomal formulation by endocytosis could evade transport mechanisms, preventing the elimination from the cell [24]. In addition, a previous study described that the TS was able to promote an increase in the influx of DOX and suppress the efflux [25].

As pHSL-TS-DOX showed advantageous *in vivo* and *in vitro* studies, we performed other *in vitro* studies to evaluate if the encapsulation of DOX could alter its activity. The apoptosis data demonstrated that both DOX and pHSL-TS-DOX are comparable, in both conditions tested, differently of npHSL-DOX-AS. Although the cumulative cell population in early and late apoptosis is similar among all the treatments, free DOX and pHSL-TS-DOX treatments showed a higher percentage of the cell population in late apoptosis than npHSL-DOX-AS. This result could suggest that the process of cell death after free DOX and pHSL-TS-DOX treatments seems to happen faster compared with npHSL-DOX-AS. Also, it is in line with the proportion of internalized DOX from the free form and pHSL-TS-DOX and the lower uptake rate obtained from npHSL-DOX-AS. Laginha et al.[13] reported that a formulation similar to npHSL-DOX-AS, when administered to 4T1 tumor-bearing mice, reached a maximum concentration in the nucleus of tumor cells after 96 h, unlike a liposomal formulation with more fluid lipid bilayer

reached in 4 h.

Free DOX and pHSL-TS-DOX induced cell cycle arrest, mainly in G1. For npHSL-DOX-AS treatment, there was a more balanced distribution between the cell division phases, and high percentage was observed in the G2-M stage. The arrest in the G1 phase suggests early detection of damage in genetic material, which gives the cells time to repair the critical damage before DNA replication occurs, avoiding the propagation of genetic lesions to progeny cells and activating the apoptotic pathway. Thus, arresting tumor cells in G1 can slow the proliferation of tumor cells [26,27]. This fact could also explain the results obtained in the study of nuclear morphology. Treatments with free DOX and pHSL-TS-DOX generated a similar percentage of normal nuclei, around 20%. Both treatments induced blocking the cell cycle at G1, which increases the probability of DNA repair mechanisms to act, and results in normal cell nuclei. On the other hand, the senescence of most cells may be due to the mechanism of action of DOX-induced DNA damage, which includes DNA alkylation, DNA cross-linking, and production of ROS [28–30].

## 5. Conclusion

The purpose of this work was to evaluate the physical properties that lead to enhanced performance of pHSL-TS-DOX compared to a similar formulation already used in the clinic. pHSL-TS-DOX presents a more fluid and permeable lipid bilayer and contains a fusogenic structural lipid, which favors the drug internalization at the cellular level to a greater extent. Also, this formulation provided higher DOX tumor accumulation. Collectively these factors are important to understand why this formulation presented a great antitumor efficacy, being stable and safe, and therefore promising for the treatment of breast cancer.

## CRediT authorship contribution statement

**Fernanda A. Boratto:** Conceptualization, Data curation, Formal analysis, Investigation, Writing – original draft. **Eduardo B. Lages:** Data curation, Investigation, Writing – review & editing. **Cristina M.C. Loures:** Data curation, Investigation, Writing – review & editing. **Adriano P. Sabino:** Data curation, Formal analysis, Writing – review & editing. **Angelo Malachias:** Data curation, Formal analysis, Writing – review & editing. **Danyelle M. Townsend:** Formal analysis, Writing – review & editing. **Andre Luis Branco De Barros:** Data curation, Formal analysis, Writing – review & editing. **Lucas Antonio Miranda Ferreira:** Conceptualization, Data curation, Formal analysis, Funding acquisition, Writing – review & editing. **Elaine Amaral Leite:** Conceptualization, Data curation, Formal analysis, Funding acquisition, Writing – review & editing.

## Declaration of Competing Interest

The authors, above cited, declare that there is no conflict of interest.

## Data Availability

Data will be made available on request.

## Acknowledgments

The authors are grateful for the support of Conselho Nacional de Desenvolvimento Cientifico e Tecnologico (CNPq-Brazil), Coordenacao de Aperfeicoamento de Pessoal de Nivel Superior (CAPES-Brazil) and Fundacao de Amparo a Pesquisa do Estado de Minas Gerais (FAPEMIG-Brazil). DMT is supported by the SC-Redox COBRE. This work was supported by the Conselho Nacional de Desenvolvimento Cientifico e Tecnologico (CNPq-Brazil) and Coordenacao de Aperfeicoamento de Pessoal de Nivel Superior (CAPES-Brazil). In addition, FERNANDA BORATTO is grateful to Fundacao de Amparo a Pesquisa do Estado de Minas Gerais (FAPEMIG-Brazil) for providing a scholarship.

## Appendix A. Supporting information

Supplementary data associated with this article can be found in the online version at doi:10.1016/j.biopha.2023.115034.

## References

[1] A.A. Wakharde, A.H. Awad, A. Bhagat, S.M. Karuppayil, Synergistic activation of doxorubicin against cancer: a review, Am. J. Clin. Microbiol Antimicrob. 1 (2) (2018) 1–6, https://doi.org/10.1016/s1734-1140(13)71021-1.
[2] Y.C. Barenholz, Doxil® – the first FDA-approved nano-drug: Lessons learned, J. Control. Release 160 (2012) 117–134, https://doi.org/10.1016/j.jconrel.2012.03.020.
[3] O. Tacar, P. Sriamornsak, C.R. Dass, Doxorubicin: an update on anticancer molecular action, toxicity and novel drug delivery systems, J. Pharm. Pharmacol. 65 (2012) 167–170, https://doi.org/10.1111/j.2042-7158.2012.01567.x.
[4] C.A. Schutz, L. Juillerat-Jeanneret, I. Lynch, M. Riediker, Therapeutic nanoparticles in clinics and under clinical evaluation, Nanomedicine 8 (2013) 449–467, https://doi.org/10.2217/nnm.13.8.
[5] M. Cagel, E. Grotz, E. Bernabeu, M.A. Moretton, D.A. Chiapetta, Doxorubicin: nanotechnological overviews from bench to bedside, Drug Discov. Today 0 (2016) 1–12, https://doi.org/10.1016/j.drudis.2016.11.05.
[6] L. Sercombe, T. Veerati, F. Moheimani, S.Y. Wu, A.K. Sood, S. Hua, Advances and challenges of liposome assited drug delivery, Front. Pharmacol. 6 (2015) 1–13, https://doi.org/10.3389/fphar.2015.00286.
[7] F.A. Boratto, M.S. Franco, A.L.B. Barros, G.D. Cassali, A. Malachias, L.A. M. Ferreira, E.A. Leite, Alpha-tocopheryl succinate improves encapsulation,pH-sensitivity, antitumor activity and reduces toxicity of doxorubicin-loaded liposomes, Eur. J. Pharm. Sci. 144 (2020), 105205, https://doi.org/10.1016/j.ejps.2019.105205.
[8] L.O.F. Monteiro, A. Malachias, G. Pound-lana, R. Magalhães-Paniago, V.C. F. Mosqueira, M.C. Oliveira, A.B. Barros, E.A. Leite, Paclitaxel-loaded pH-sensitive liposome: new insights on structural and physicochemical characterization, Langmiur 34 (2018) 5728–5737, https://doi.org/10.1021/acs.langmuir.8b00411.
[9] X. Guan, Y. Li, Z. Jiao, J. Chen, Z. Guo, H. Tian, X. Chen, A pH-sensitive charge-conversion system for doxorubicin delivery, Acta Biomater. 9 (2013) 7672–7678, https://doi.org/10.1016/j.actbio.2013.04.047.
[10] D.S. Ferreira, S.C.A. Lopes, M.S. Franco, M.C. Oliveira, pH sensitive liposomes for drug delivery in cancer treatment, Ther. Deliv. 4 (2013) 1099–1123, https://doi.org/10.4155/tde.13.80.
[11] S.V. Mussi, G. Parekh, P. Pattekari, T. Levchenko, Y. Lvov, L.A.M. Ferreira, V. Torchilin, Improved pharmacokinetics and enhanced tumor growth inhibition using a nanostructured lipid carrier loaded with doxorubicin and modified with a layer-by-layer polyelectrolyte coating, Int J. Pharm. 495 (1) (2015) 186–193, https://doi.org/10.1016/j.ijpharm.2015.08.079.
[12] K.M. Laginha, S. Verwoert, G.J.R. Charrois, T.M. Allen, Determination of doxorubicin levels in whole tumor and tumor nuclei in murine breast cancer tumors, Clin. Cancer Res 11 (2005) 6944–6949, https://doi.org/10.1158/1078-0432.CCR-05-0343.
[13] M.S. Franco, M.C. Roque, A.L.B. Barros, J.O. Silva, G.D. Cassali, M.C. Oliveira, Investigation of the antitumor activity and toxicity of long-circulating and fusogenic liposomes co-encapsulating paclitaxel and doxorubicin in a murine breast cancer animal model, Biomed. Pharm. 109 (2019) 1728–1739, https://doi.org/10.1016/j.biopha.2018.11.011.
[14] B. Heurtault, P. Saulnier, B. Pech, J.E. Proust, J.P. Benoit, Physico-chemical stability of colloidal lipid particles, Biomat 24 (2003) 4283–4300, https://doi.org/10.1016/S0142-9612(03)00331-4.
[15] E.C. Filippi-Chiela, M.M. Oliveira, B. Jurkovski, S.M. Callegari-Jacques, V.D. da Silva, G. Lenz, Nuclear morphometric analysis (NMA): screening of senescence, apoptosis and nuclear irregularities, Plos One 7 (8) (2012), e42522, https://doi.org/10.1371/journal.pone.0042522.
[16] A. Gabizon, H. Shmeeda, Y. Barenholz, Pharmacokinetics of pegylated liposomal doxorubicin - Review of animal and human studies, Clin. Pharm. 42 (5) (2003) 419–436, https://doi.org/10.2165/00003088-200342050-00002.
[17] H. Xu, L. Zhang, L. Li, Y. Liu, Y. Chao, X. Liu, Z. Jin, Y. Chen, X. Tang, H. He, Q. Kan, C. Cai, Membrane-loaded doxorubicin liposomes based on ion-pairing technology with high drug loading and pH-responsive property, AAPS Pharm. Sci. Tech. 18 (2017) 2120–2130, https://doi.org/10.1208/s12249-016-0693-x.
[18] S. Sindhwani, A.M. Syed, J. Ngai, B.R. Kingston, L. Maiorino, J. Rothschild, P. MacMillan, Y. Zhang, N.U. Rajesh, T. Hoang, J.L.Y. Wu, S. Wilhelm, A. Zilman, S. Gadde, A. Sulaiman, B. Ouyang, Z. Lin, L. Wang, M. Egeblad, W.C.W. Chan, The entry of nanoparticles into solid tumours, Nat. Mater. 19 (2020) 566–575, https://doi.org/10.1038/s41563-019-0566-2.
[19] P. Yingchoncharoen, D.S. Kalinowski, D.R. Richardson, Lipid-based drug delivery systems in cancer therapy: what is available and what is yet to come, Pharm. Rev. 68 (2016) 701–787, https://doi.org/10.1124/pr.115.012070.
[20] R. Kolasinac, C. Kleusch, T. Braun, R. Merkel, A. Csiszar, Deciphering the functional composition of fusogenic liposomes, Int J. Mol. Sci. 19 (2018) 1–15, https://doi.org/10.3390/ijms19020346.
[21] C.M. Dawidczyk, L.M. Russel, M. Hultz, P.C. Searson, Tumor accumulation of liposomal doxorubicin in three murine models: Optimizing delivery efficiency,

Nanomed.: Nanotechnol. Biol. Med. 13 (2017) 1637–1644, https://doi.org/10.1016/j.nano.2017.02.008.
[22] A. Akbarzadeh, R. Rezaei-Sadabady, S. Davaran, S.W. Joo, N. Zarghami, Y. Hanifehpour, M. Samiei, M. Kouhi, N. Nejati-Koshki, Liposome: classification, preparation, and applications, Nanoscale Res Lett. 8 (2013) 1–9, https://doi.org/10.1186/1556-276X-8-102.
[23] R.M. Epand, N. Fuller, R.P. Rand, Role of the position of unsaturation on the phase behavior and intrinsic cuvature of phosphatidylethanolamines, Biophys. J. 71 (1996) 1806–1810, doi:0006-3495/96/10/1806/05.
[24] G. Bozzuto, A. Molinari, Liposomes as nanomedical devices, Int J. Nanomed. 10 (2015) 975–999, https://doi.org/10.2147/IJN.S68861.
[25] X. Zhang, X. Peng, W. Yu, S. Hou, Y. Zhao, Z. Zhang, X. Huang, K. Wu, Alpha-tocopheryl succinate enhances doxorubicin-induced apoptosis in human gastric cancer cells via promotion of doxorubicin influx and suppression of doxorubicin efflux, Cancer Lett. 307 (2011) 174–181, https://doi.org/10.1016/j.canlet.2011.04.001.
[26] L.C. Maroni, A.C.O. Silveira, E.A. Leite, M.M. Melo, A.F.C. Ribeiro, G.D. Cassali, C. M. Souza, E.M. Souza-Fagundes, I.R. Caldas, M.S. Araujo, A.O. Martins-Filho, M. C. Oliveira, A. Teixeira-Carvalho, Antitumor effectiveness and toxicity of cisplatin-loaded long-circulating and pH-sensitive liposomes against Ehrlich ascitic tumor, Exp. Biol. Med. 237 (2012) 973–984, https://doi.org/10.1258/ebm.2012.011432.
[27] L.O.F. Monteiro, R.S. Fernandes, L. Castro, D. Reis, G.D. Cassali, F. Evangelista, C. Loures, A.P. Sabino, V. Cardoso, M.C. Oliveira, A.B. Barros, E.A. Leite, Paclitaxel-loaded folate-coated ph-sensitive liposomes enhance cellular uptake and antitumor activity, Mol. Pharm. 16 (2019) 3477–3488, https://doi.org/10.1021/acs.molpharmaceut.9b00329.
[28] A. Bielak-Zmijewska, M. Wnuk, D. Przybylska, W. Grabowska, A. Lewinska, O. Alster, Z. Korwek, A. Cmoch, A. Myszka, S. Pikula, G. Mosieniak, E. Sikora, A comparison of replicative senescence and doxorubicin-induced premature senescence of vascular smooth muscle cells isolated from human aorta, Biogerontology 15 (2014) 47–64, https://doi.org/10.1007/s10522-013-9477-9.
[29] D.A. Gewirtz, A critical evaluation of the mechanisms of action proposed for the antitumor effects of the anthracycline antibiotics adriamycin and daunorubicin, Biochem Pharm. 57 (1999) 727–741, https://doi.org/10.1016/s0006-2952(98)00307-4.
[30] L.W. Elmore, C.W. Rehder, X. Di, P.A. McChesney, C.K. Jackson-Cook, D. A. Gewirtz, S.E. Holt, Adriamycin-induced senescence in breast tumor cells involves functional p53 and telomere dysfunction, J. Biol. Chem. 277 (2002) 35509–35515, https://doi.org/10.1074/jbc.M205477200.